View metadata, citation and similar papers at core.ac.uk

brought to you by CORE

provided by NASA Technical Reports Server

860207

Received 18 July 1986

NGL 05-002-134
IN- 31521

26 P.

Spectroscopy of the Globular Clusters in M87

J.R. Mould, J.B. Oke, and J.M. Nemec

Palomar Observatory, Caltech 105-24, CA 91125

Abstract

With a velocity dispersion of 370 ± 50 km/sec the globular cluster system of M87 is kinematically hotter than the stars in the giant elliptical itself. This is consistent with the clusters' shallower density distribution for isotropic orbits. The mean metallicity of the 27 clusters in the sample analyzed here is no more than a factor of 2 more metal rich than the cluster system of the Milky Way, but considerably more metal poor than the integrated starlight in the field at a radius of 1′ from the center of M87. There is no evidence for the existence of young clusters in the system. The mass-radius relation between 1′ and 5′ required to contain the globular clusters joins on to that required to contain the hot gas around M87.

I. Introduction

Globular clusters are the only structures with a proven origin early in the history of the Universe. Since they probably reflect conditions during the collapse and formation of galaxies, it is important to study their physical and chemical composition in galaxies of a range of morphology. In addition, the kinematics of globular clusters offer a basis for comparing the masses of galaxies over the length of the Hubble sequence, not available with other tracers of the gravitational potential.

In this paper we report the first results of a study of the globular cluster system of M87. How the spectra were obtained is indicated in §II; §III describes the redshift distribution of the sample studied. A spectral classification is presented in §IV. In §V we determine the cluster velocity dispersion as a function of radius and attempt to understand why it is higher than that of the integrated light of M87. The metallicity distribution of the cluster system is compared in §VI with that of the Milky Way and found to be similar. Finally we discuss the implications for formation scenarios (§VII) and the mass of M87 (§VIII).

II. Observations

The study by Strom *et al.* (1981) of the photometric properties and distribution of M87's cluster system forms the basis of the present work. Strom *et al.* list 1728 objects centered on M87 within $1.5' < r < 9.0'$ (the central hole being due to photographic limitations in background subtraction). The limiting magnitude is B = 23.5. For the present purposes we selected groups of brighter objects to fall optimally on an array of 8 parallel aluminized quartz slides, which constitute the multislit assembly of the 5-m telescope Double Spectrograph (Oke and Gunn 1982). The astrometric study by Prociuk (1976) was consulted in choosing the fields to observe, although not all objects with measureable proper motion were excluded from the sample.

Each slit of the mulitslit assembly was 15″ in length and 1″ wide and able to be translated in the dispersion direction ±30″, giving access to a field 2′ x 1′. If M87 is at distance modulus 31.1 (Aaronson and Mould 1983), 1′ is equivalent to 5 kpc. On the blue side of the instrument we used a 300 line grating blazed at 4000 $\AA$, giving a resolution of 2.1 $\AA$/pixel on a Texas Instruments CCD. Spectra of similar $\Delta\lambda/\lambda$ were obtained on the red side, but are not discussed here.

Three half-nights in May 1985 and three nights in March 1986 were sufficient to secure spectra of 52 objects with B < 22 in 10 fields with exposure times of 12000 seconds per field. For fainter objects, in average seeing, less than 100 counts per channel were recorded above sky, resulting in a signal to noise ratio too low for accurate radial velocities (see below). To protect against the effects of spectrograph flexure and cosmic ray detection, these long exposures were accumulated from individual 3000 second exposures. In general we found no problem with flexure at the 20 km/sec level and simply extracted the object spectra using normal interpolative sky subtraction techniques (Boroson and Oke 1982). These were then combined, either taking the median spectrum to null out cosmic ray hits, or averaging and editing trouble-spots.

The spectrum of cluster 547 of Strom *et al.* (after four point Gaussian smoothing) is shown in Figure 1 . This is one of the highest S/N spectra we have obtained. No flux calibration has been applied.

III. Redshift Distribution

The unsmoothed spectra were rebinned on to a logarithmic wavelength scale and cross-correlated against IAU radial velocity standards of F, G and K type. These stars together with observations of Galactic globular clusters (which were drifted across the spectrograph slit) provided the velocity zeropoint. The r.m.s. error in the radial velocities of these bright standard objects was 30 km/sec. Clusters 501 and 582 were reobserved in the second year with a different multislit geometry, and the r.m.s. error was 40 km/sec.

A considerable amount of testing was done to determine the size of the errors on faint objects. By working with the uncombined spectra and the standard template, we learned that when the height of the cross-correlation peak fell as low as 0.14, the velocity uncertainty of the combined spectrum was approximately 100 km/sec, and increased rapidly with declining peak height. Heliocentric radial velocities are reported in Table 1 for 43 objects; 9 others failed the peak height criterion.

IV. Assignment of Spectral Types

A simple minded spectral type is included in Table 1 (column 2). We have designated "Cl" for cluster any spectrum whose velocity falls between 300 and 2500 km/sec. This interval corresponds to ± 3 times the velocity dispersion of the objects within the interval. There are 27 such clusters in Table 1. Two objects are classified "F" type for their strong hydrogen lines and velocity less than 300 km/sec. Objects with velocity larger than 2500 km/sec we have designated "G" for background galaxy; there are 4 of them. There are also 4 "K" stars, classified by the criterion $v < 300$ km/sec and a strong MgH band. "M" type spectra have $v < 300$ km/sec and strong TiO bands. Since no template M star was observed, the net positive velocity of the 6 M stars is probably not real. As indicated earlier, there are 9 objects with cross-correlation peaks less than 0.14; 7 of these which appear to have velocities exceeding 2500 km/sec are designated "G?" and the other two are classified "?".

Also included in Table 1 are the U-B color of the objects given by Strom *et al.* (1981) (column 3) and an index of the strength of the Mg b lines in the spectra (column 4). The MgB index is defined in a similar way to the Mg_2 index of Burstein *et al.* (1984), and, according to our observations of M92, M3 and NGC6356, transforms to it by the addition of 0.06 ± 0.01 mag.

V. The Velocity Dispersion

The mean radial velocity of the 27 clusters in Table 1 is 1320 ± 70 km/sec. This is not significantly different from the heliocentric velocity of M87, which is 1265 ± 15 km/sec in the CfA catalog (Huchra *et al.* 1983). Their velocity distribution is shown in Figure 2 and compared with a gaussian with the same velocity dispersion, namely 370 ± 50 km/sec. The data are still so few that any differences are obviously insignificant. Since 100 km/sec is an upper limit on individual errors, correction of the velocity dispersion for measurement errors is unnecessary. There is no evidence for rotation of the globular cluster system, but the distribution of the sample on the sky is not suitable for setting tight constraints on rotation at the present time. The best that can be done now is to compare the mean cluster velocity on one side of the minor axis with the redshift of the galaxy, which yields an upper limit of 150 km/sec on a flat cluster rotation curve amplitude.

It is of interest to examine the run of velocity dispersion with radius, so the data were binned in radius for this purpose. The binned data are summarized in Table 2. The velocity dispersion profile is plotted in Figure 3 and compared with measurements on the integrated light of M87 by Sargent *et al.* (1978). There is almost no overlap between the two data sets, but if we extend the data from the integrated starlight using a constant M/L, constant anisotropy model (the dashed line), it is clear that the globular cluster velocity dispersion profile is different from this extension in a significant way. As we show below, this behavior is to be expected as a consequence of the different density profiles of the clusters and the starlight.

In terms of Binney's anisotropy parameter $\beta = (\sigma_r^2 - \sigma_\theta^2)/\sigma_r^2$ (Binney and Mamon 1982) the equation of stellar hydrodynamics for a spherical galaxy is:

$$\sigma_r^2[\frac{d\ ln\ \rho}{d\ ln\ r} + \frac{d\ ln\ \sigma_r^2}{d\ ln\ r} + 2\beta] = -\frac{GM(r)}{r}$$

Here $M(r)$ is the total mass within radius r, and ρ is the density of test objects with radial velocity dispersion σ_r and azimuthal dispersion σ_θ. The surface density $\Sigma_{stars} \propto r^{-2.2}$ while $\Sigma_{globs} \propto r^{-1.1}$ according

to Grillmair, Pritchet and van den Bergh (1986), so that the corresponding volume densities are approximately $\rho_{stars} \propto r^{-3.2}$ and $\rho_{globs} \propto r^{-2.1}$. Thus:

$$\frac{\sigma_r^2(globs)}{\sigma_r^2(stars)} = \frac{2\beta_{stars}-3.2}{2\beta_{globs}-2.1} \quad = 1.5 \text{ if } \beta = 0.$$

Here we have neglected the middle term on the LHS of the hydrodynamical equation as it is small compared with the first term even in the model with constant M/L. We have also neglected rotation, which contributes an additional smaller term $(v_{rot}/\sigma_r)^2$. Davies *et al.* (1983) quote $v_{max}/\sigma < 0.07$ for M87's integrated light and $\epsilon = 0.14$. The ellipticity of the cluster system could be as high as 0.3 or as low as 0, judging from counts by Harris and Smith (1976) and Grillmair *et al.* (1986), but $v_{rot}/\sigma < 0.4$, according to our estimates in the previous section, which justifies its neglect.

The quantity σ_r is the radial velocity dispersion as distinct from σ_v, the line of sight velocity dispersion. For σ_r = constant, it is easily shown that the adopted density laws project to:

$$\frac{\sigma_v^2(globs)}{\sigma_v^2(stars)} = \frac{2\beta_{stars}-3.2}{2\beta_{globs}-2.1} \; \frac{1-\beta_{globs}/2}{1-2\beta_{stars}/3} \quad = 1.5 \text{ if } \beta = 0$$

Sargent *et al* (1978) find:

$$\sigma_v(stars) = 278 \pm 11 \text{ km/s for } 10'' < r < 42''.$$

On this basis we would expect:

$\sigma_v(globs) = 343$ km/s from the shallower cluster distribution if $\beta = 0$. This value would increase if $\beta > 0$. We find:

$$\sigma_v(globs) = 370 \pm 50 \text{ km/s for } 1' < r < 6'.$$

The critical observation here is the shallower distribution populated by the globular clusters than M87's field stars. Lauer and Kormendy (1986) have observed a similar phenomenon in the central parts of M87, where a core radius of the cluster system is detected and shown to be larger than that of the integrated light. In the outer parts ($r > 4'$) Harris (1986) found $\Sigma(globs) \propto r^{-1.6}$, steeper than determined by Grillmair *et al.*, but still significantly different from the galaxy surface brightness distribution at those radii.

One can also in principle understand our ratio of $\sigma_v(globs)/\sigma_v(stars)$, if we suppose $\beta_{globs} > 0$. The Binney and Mamon (1982) model has $\beta_{stars} < 0.2$ for r > 40″, which has a negligible effect on the velocity dispersion ratio. But if we suppose β_{globs} is small but positive at large radii, then $\sigma_v^2(globs)/\sigma_v^2(stars) \simeq 1.5\ (1 + \beta_{globs}/2)$. Thus $\sigma_v(globs)/\sigma_v(stars) = 1.3$ for $\beta_{globs} = 0.25$, for example.

VI.The Metallicity Distribution

The distribution of U-B colors for the available objects in Table 1 is shown in Figure 4. It is apparent that the removal of contaminating red and blue objects narrows the cluster color distribution considerably, so that it looks rather similar to that of the globular clusters in the Milky Way (tabulated by Harris and Racine 1979). To test the similarity of the distributions, rather than concern ourselves with the identity of ultraviolet photometric systems and questions of Galactic reddening, we shall examine the cluster Mg indices presented here.

Figure 5 shows the correlation between MgB and U-B from Table 1. Based on repeatability of the indices of two of the brighter clusters, the r.m.s. errors in MgB are at least as large as 0.03 mag. The existence of a good correlation in Figure 5 indicates that the U-B color dispersion in M87 results from a metallicity range in the cluster system, as is the case for that of the Milky Way. In addition, we show in Figure 5 two points representative of the integrated light of M87 at 1′ radius from the center. These measurements were made from the background light falling on the slit closest to the center of M87, after subtraction of the light falling on the most distant slit, which is mostly night sky. These two samples are

plotted at the U-B value corresponding to that radius from Strom *et al.*. It is clear that the starlight at 1′ is as metal rich as any of the globular clusters in the present sample.

The mean value of MgB for the cluster sample is 0.033 ± 0.017. If this value is converted to the Mg_2 scale, as indicated above, one can employ a linear transformation of Mg_2 to Zinn's (1985) [Fe/H]. The result is $<[Fe/H]> = -1.2 \pm 0.2$ for clusters with $r > 2r_e/3$ in M87. This compares with $<[Fe/H]> = -1.4 \pm 0.05$ for Milky Way clusters with $r > 2$ kpc. The sources of the effective radii on which this comparison is based are de Vaucouleurs and Nieto (1978) and de Vaucouleurs (1977). Since the calibration of Mg_2 to [Fe/H] is only really well established in the interval (-2,-1) in metallicity, it is worth comparing the median values of M87 and Galactic MgB indices. The median metallicity depends only on the cluster ranking and not on the calibration outside its range of validity. However, the median metallicities turn out to be the same as the means within the quoted errors. We conclude that the chemical composition of our sample of 27 outer clusters in M87 is no more than a factor of two richer in heavy elements than that of the halo cluster population of the Milky Way.

This result is consistent with the appearance of Figure 4, but is contrary to the conclusion of Hanes and Brodie (1986), who find $<[Fe/H]> = -0.5 \pm 0.4$ for a sample of 6 objects. We have observed the three most metal rich of their clusters, III-122 (= Cl 1584), III-172 (= Cl 1093), and IV-94 (=Cl 784). The average MgB index of these clusters is comparable with that of NGC6356, according to our observations, but [Fe/H] = 0.3 for the first two clusters, and -0.1 for the third, according to Hanes and Brodie; so the difference would seem to be in the measurements or calibration rather than just the sample.

Strom *et al.* (1981) found that the integrated light of M87 is redder than that of the globular clusters at any radius. The comparison of line strengths presented here is qualitatively consistent with that result and points to metallicity differences as the source of the color difference. It is desirable to go further than that and estimate the metallicity difference between the clusters and the field at any radius, but difficult with the present limited data. A glance at Table 2 shows that we do not even detect the metallicity gradient

in the cluster system. But, given the uncertainties, the data are not inconsistent with the gradient detected by Strom *et al.* in U-B. If we compare MgB(stars) = 0.20 with the clusters of the first bin of Table 2, the difference is significant (0.23 ± 0.1 in δMgB). If the U-B gradient is forced through the combined MgB data of Table 2, the extrapolation yields MgB(globs) = 0.06 ± 0.03 at 1′, which corresponds to [Fe/H] = -0.9. To estimate the field metallicity at 1′, we should not extrapolate the globular cluster calibration (see Burstein 1979). However, the measured Mg index in this case is approximately equal to the value in the nucleus of M31, for which Mould (1978) obtained [Fe/H] = 0.1. So, at 1′ we estimate that the clusters are approximately 1.0 dex more metal poor than the integrated light. Strom *et al.* (1981) found 0.6 dex from δ(U-V).

Finally, we have examined the relation between cluster luminosity and U-B or MgB. There is no apparent correlation beyond the brightest and faintest points. But only 3 mag in luminosity have been sampled, and a larger sample with a larger range is required to test the possibility that the most massive clusters are self-enriched.

VII. Discussion

Two properties of the present sample, the metal abundance distribution and the lack of any trend of metallicity with luminosity, indicate a basic similarity of the M87 cluster system to the better known systems of the Milky Way and M31. This similarity can tentatively be extended to the age distribution, as no M87 clusters are seen with hydrogen line strengths as strong as Searle, Wilkinson and Bagnuolo (1980) type V or earlier clusters in the Magellanic Clouds. One or two clusters appear to have anomalously strong $H\beta$ in the same degree as is seen in the M31 sample of Burstein *et al.* (1984). We conclude that as stellar populations the cluster systems of M87, M31 and the Milky Way are basically similar[1]: all three are ancient, metal poor, pressure supported systems.

[1] This similarity extends, for example, to the larger effective radius found for the globular cluster system compared to the bulge in M31 (Walterbos 1986). A fuller comparison (for example with the well placed cluster system in NGC5128; see Hesser *et al.* 1984) would be of interest, but is outside the scope of the present paper.

The surprising properties of the M87 cluster system (aside from the sheer number of clusters) are its different radial distribution from the rest of the galaxy and the distinct metallicity of clusters from that of their local field. One theory which naturally explains the phenomena in the context of galaxy formation is discussed by Fall and Rees (1985). Fall and Rees note that a thermal instability in the infall of hot gas into a protogalactic potential will promote the formation of $10^6 M_\odot$ structures of $10^{-2} Z_\odot$ metallicity at early times. The formation of field stars and clusters less massive than $10^6 M_\odot$ should be inhibited until Z is of order $10^{-1} Z_\odot$. The lack of 10^9 year old clusters in the present sample would suggest that this process is *not* still continuing in the hot gas currently surrounding M87. In the Fall and Rees theory one would not expect continuing massive cluster formation in gas of the high metallicity observed in the x-rays. The low mean metallicity reported here for the clusters is additional evidence that the bulk of them did not form from the gas in its present state. On the contrary, early cluster formation may have played an important role in enriching the gas according to considerations discussed by De Young *et al.* (1983).

A second possibility which deserves consideration is that M87, as a central cluster galaxy, may have received a major contribution from the merger of gas rich subgalaxies containing globular clusters. Subsequent dissipation in the gaseous component would concentrate and enrich the elliptical-to-be, but the clusters would retain their initial kinetic energy and metallicity. Our finding that there is nothing special about the overall chemical properties of the cluster system of this singular galaxy enhances this possibility. In this case the lack of 10^9 year old clusters in the present sample does not put limits on the ongoing nature

of the accretion process. Harris (1986), however, points out that ellipticals in small groups also seem to show cluster systems looser than they are themselves. So the dynamical environment of the galaxy does not seem to play a key role in the process. The existence of a color gradient suggests that mergers are only part of the story of the formation of the M87 globular cluster system.

It is certainly too early to judge which of these or other scenarios discussed by Harris (1986) may be responsible for the different properties of the clusters and the stars in M87. For the time being we simply note that, in addition to being less centrally concentrated and bluer, the cluster system is kinematically hotter and more metal poor than the body of the galaxy. These are the properties that we normally use to distinguish stellar populations, and in this sense the cluster system of M87 is a more primitive population than the field stars which contribute most of the light. This was the main conclusion of the pioneering work of Strom *et al.* (1981), and the present paper just provides the kinematic complement to that and other studies discussed earlier.

VIII. The Mass Distribution

It is clear from Figure 3 that a cluster velocity dispersion that is constant with radius is consistent with the data to 6′. But the error bars will also permit a falling velocity dispersion with radius, corresponding to a constant M/L model. Hence the present data cannot by themselves be used to make a strong case for dark matter in ellipticals. (With double the sample size we expect to be able to do this.) However, if we assume constant $\sigma(r)$, zero anisotropy and the radial distribution quoted earlier, we obtain $M(r) = 2.1 r\sigma^2/G$ $= 3 \times 10^{11}$ r (arcmin) $M_\odot$ with M87 at a distance of 15 Mpc.

Figure 6 shows the mass distribution around M87 inferred from the x-ray emitting gas centered on M87. The form of the mass model is taken from the detailed discussion by Fabricant and Gorenstein (1983) (see their paper for a number of prior references). The large inferred mass is required to contain the hot gas. Containment is required since the observed mass of gas is large compared with any plausible production

rate. Hydrostatic equilibrium is therefore used to model what is more precisely referred to as a quasistatic cooling flow.

The present data smoothly join the mass-radius relation required to "contain" the integrated starlight (Sargent *et al.* 1978) to the mass-radius relation required to contain the gas. The latter relation becomes less certain at small radii because of the difficulty of determining the temperature profile in the gas within 3′ of the center of M87 (Fabricant and Gorenstein 1983). Figure 6 emphasizes the unity of the gravitational potential which contains the starlight, clusters and x-ray gas. It does not answer the more difficult (but possibly semantic) question of whether the mass distribution in M87 is separable in some way from the gravitational potential of the core of the Virgo cluster.

IX. Conclusions

We have obtained multi-slit spectra of a total of 52 objects lying within 7′ of the center of M87. The principal conclusions are as follows:

1. Twenty-seven of the objects are globular clusters with a mean heliocentric radial velocity of 1320 km/sec and a dispersion of 370 ± 50 km/sec.

2. Of the remaining objects 12 are subdwarf stars; 4 are definitely (and 7 are probably) background galaxies; and 2 are unclassified.

3. For the clusters the Mg index is well correlated with U-B color and follows the relation for Galactic globular clusters, proving that a metallicity spread is the source of the color dispersion.

4. At 1′ radius the integrated light of M87 is as strong lined as the most metal rich clusters in the sample, in qualitative agreement with the results of Strom *et al.* (1981).

5. The red tail of the color distribution of the complete sample consists of red dwarfs; the blue tail consists of F and G subdwarfs and background galaxies. Removal of the contaminating objects narrows the U-B distribution of the sample, so that it is similar in shape and no more than 0.1 mag redder than that of the Galaxy. Based on the Mg index alone, for $r > 2r_e/3$, the mean metallicity of M87 globular clusters exceeds that of the Milky Way by no more than 0.3 dex (1 σ).

6. The velocity errors are 30 km/sec on bright objects and approach 100 km/sec at B = 21.5 with a total of 12000 seconds exposure time .

7. The cluster data are consistent with $\sigma(r)$ = constant. But the sample size must be doubled to exclude M/L = constant at the 95% confidence level.

8. If $\sigma(r)$ = constant, $\sigma_{globs} / \sigma_{stars} = 1.4 \pm 0.2$ at 1′. For isotropic orbits this is consistent with the greater radial concentration of the starlight.

9. If $\sigma(r)$ = constant, $\beta = 0$ and $\rho \propto r^{-2.1}$,

$$M(r) = 6 \times 10^{10} \text{ r (kpc) } M_\odot$$

$$= 3 \times 10^{11} \text{ r (arcmin) } M_\odot$$

This mass-radius relation makes the connection between previous optical studies and that inferred from the need to contain the hot x-ray gas around M87.

It is a pleasure to acknowledge profitable discussions with Ray Carlberg, Rebecca Elson, Mike Fall, Wal Sargent, Paul Schechter and Rosie Wyse on the M87 globular clusters. We are obliged to Sidney van den Bergh for drawing attention to Prociuk's useful proper motion study of M87. JRM would like to thank the Space Telescope Science Institute for their hospitality during the writing of this paper. We

gratefully acknowledge the partial support of this project by NASA grant NGL-05-002-134 and NSF grant AST-8502518.

References

Aaronson, M. and Mould, J. 1983, *Ap.J.*, **265**, 1.

Binney, J. and Mamon,G. 1982, *M.N.R.A.S.*, **200**, 361.

Boroson, T., Oke, J.B. and Green, R. 1982, *Ap.J.*, **263**, 32.

Burstein, D. 1979, *Ap.J.*, **232**, 74.

Davies, R., Efstathiou, G., Fall, S.M., Illingworth, G. and Schechter, P. 1983, *Ap.J.*, **266**, 41.

Burstein, D., Faber, S.M., Gaskell, C.M. and Krumm, N. 1984, *Ap.J.*, **287**, 586..

de Vaucouleurs, G. 1977, *A.J.*, **82**, 456.

de Vaucouleurs, G. and Nieto, J.-L. 1978, *Ap.J.*, **220**, 449.

De Young, D., Lind, K. and Strom, S.E. 1983, *Pub. A.S.P.*, **95**, 401.

Fabricant, D. and Gorenstein, P. 1983, *Ap.J.*, **267**, 535.

Fall, S.M. and Rees, M. 1985, *Ap.J.*, **298**, 18.

Grillmair, C., Pritchet, C. and van den Bergh, S. 1986, *A.J.*, **91**, 1328.

Hanes, D. and Brodie, J. 1986, *Ap.J.*, **300**, 279.

Harris, W. 1986, *A.J.*, **91**, 822.

Harris, W. and Racine, R. 1979, *Ann.Rev.Astr.Ap.*, **17**, 241.

Harris, W. and Smith, M. 1976, *Ap.J.*, **207**, 1036.

Hesser, J.E., Harris, H.C., van den Bergh, S. and Harris, G.L.H. 1984, *Ap.J.*, **276**, 491.

Huchra, J., Davis, M., Latham, D. and Tonry, J. 1983, *Ap.J.Suppl.*, **52**, 89.

Lauer, T. and Kormendy, J. 1986, *Ap.J. Letters*, **303**, L1.

Mould, J. 1978, *Ap.J.*, **220**, 434.

Oke, J.B. and Gunn, J. 1982, *P.A.S.P.*, **94**, 586.

Prociuk, I. 1976, M.Sc. thesis, University of Toronto

Sargent, W., Young, P., Boksenberg, A., Shortridge, K., Lynds, C.R. and Hartwick, F.D.A. 1978, *Ap.J.*, **221**, 731.

Searle, L., Wilkinson, A. and Bagnuolo, W. 1980, *Ap.J.*, **239**, 803.

Strom, S., Forte, J.C., Harris, W., Strom, K., Wells, D. and Smith, M. 1981, *Ap.J.*, **245**, 416.

Walterbos, R. 1986, Ph.D. thesis, University of Leiden.

Zinn, R. 1985, *Ap.J.*, **293**, 424.

Table 1: Spectroscopy of M87 Globular Clusters

Object No.[1]	Type	Velocity km s^{-1}	U-B mag	MgB arcmin	Radius
206	G?	11095	0.12	–	7.8
207	Cl	1645	0.04	-0.00	8.0
218	M	90	1.18	–	7.3
236	F	25	-0.06	–	6.8
293	M	115	–	–	6.5
296	K	-20	–	–	6.1
444	G	0.268[2]	-0.14	–	3.1
468	Cl	1240	0.46	0.15	4.0
501	Cl	1940	0.20	0.01	3.7
503	F	0	-0.02	–	2.6
547	Cl	765	0.68	0.10	3.0
582	Cl	1530	0.18	0.00	3.5
601	G	2735	0.13	–	1.9
645	Cl	1740	0.41	0.21	1.7
668	Cl	1510	0.29	0.07	2.8
670	M	160	1.09	–	2.3
697	?	1360	–	–	1.3
684	Cl	1430	0.15	-0.07	3.3
708	Cl	1130	-0.08	0.12	2.9
720	K	210	0.81	–	2.5
740	?	935	0.14	–	2.5
784	Cl	1940	0.28	0.11	3.3
789	Cl	795	0.18	-0.14	1.7
797	G	2925	-0.10	–	3.0
804	Cl	1170	0.40	0.15	2.7
829	Cl	835	0.00	-0.05	2.0
831	Cl	1080	0.17	0.00	3.9
835	M	120	–	–	3.5
838	Cl	1155	0.16	-0.06	2.4
854	G?	7000	-0.09	–	4.3
928	Cl	1309	–	0.00	1.1
939	G	5150	-0.12	–	1.5
941	G?	13160	0.10	–	4.2
944	G?	14000	–	–	3.8
965	Cl	1465	0.32	0.05	4.2
969	G?	6310	0.41	–	2.6
991	Cl	1025	0.03	0.04	3.3
999	Cl	1515	0.11	-0.17	1.8
1019	Cl	725	0.24	-0.03	4.6
1034	Cl	1005	0.31	0.05	4.4
1039	G?	22430	0.15	–	2.1
1044	Cl	2065	0.10	-0.05	3.1
1093	Cl	930	0.40	0.05	4.8

1103	F	95	-0.08	–	2.2
1109	K	25	0.38	–	2.3
1155	Cl	1385	0.59	0.13	2.8
1219	G?	16285	0.20	–	2.9
1549	M	275	1.19	–	4.9
1584	Cl	1340	0.39	0.10	5.4
1608	M	135	1.09	–	5.9
1615	Cl	1405	0.18	0.04	5.8
1631	Cl	1545	0.14	0.06	6.4

Notes to Table 1:

[1] From Strom *et al.* (1981).

[2] This is the absorption line redshift; λ3727 is present in emission at this redshift.

Table 2: Cluster Properties within 4 radial bins

Radius arcmin	$< v >$ km/s	σ km/s	<MgB> mag	δMgB mag	n
1-2	1340	405	-0.03	±0.09	4
2-3	1135	270	0.07	±0.03	7
3-4	1575	425	0.01	±0.02	7
4-8	1255	310	0.05	±0.02	9

Figure Captions

Figure 1 The spectrum of Cl 547 in M87. The data have been smoothed from the original resolution. The vertical axis shows detected photons.

Figure 2 The radial velocity distribution of objects classified as clusters in Table 1.

Figure 3 Velocity dispersion profile of M87 globular clusters (solid symbols) and integrated starlight. The dashed line is a constant M/L model fitted to the data of Sargent *et al.* (1978) at small radii. The solid line is a constant σ fit to the cluster data.

Figure 4 The color distribution of objects classified as clusters in Table 1 (shaded histogram), compared with the corresponding distribution for Galactic globular clusters. The influence of other contaminating objects on the M87 distribution is shown.

Figure 5 The relation between MgB index and the U-B colors of Strom *et al.* (1981) for M87 clusters (solid symbols). Open circles show our measurements of M92, M3 and NGC6356. The boxes show the strong MgB features of the integrated starlight 1′ from the center of the galaxy.

Figure 6 The mass radius relation obtained in the present work between 1′ and 6′ smoothly joins that from previous optical data to that required to contain the x-ray emitting gas around M87.

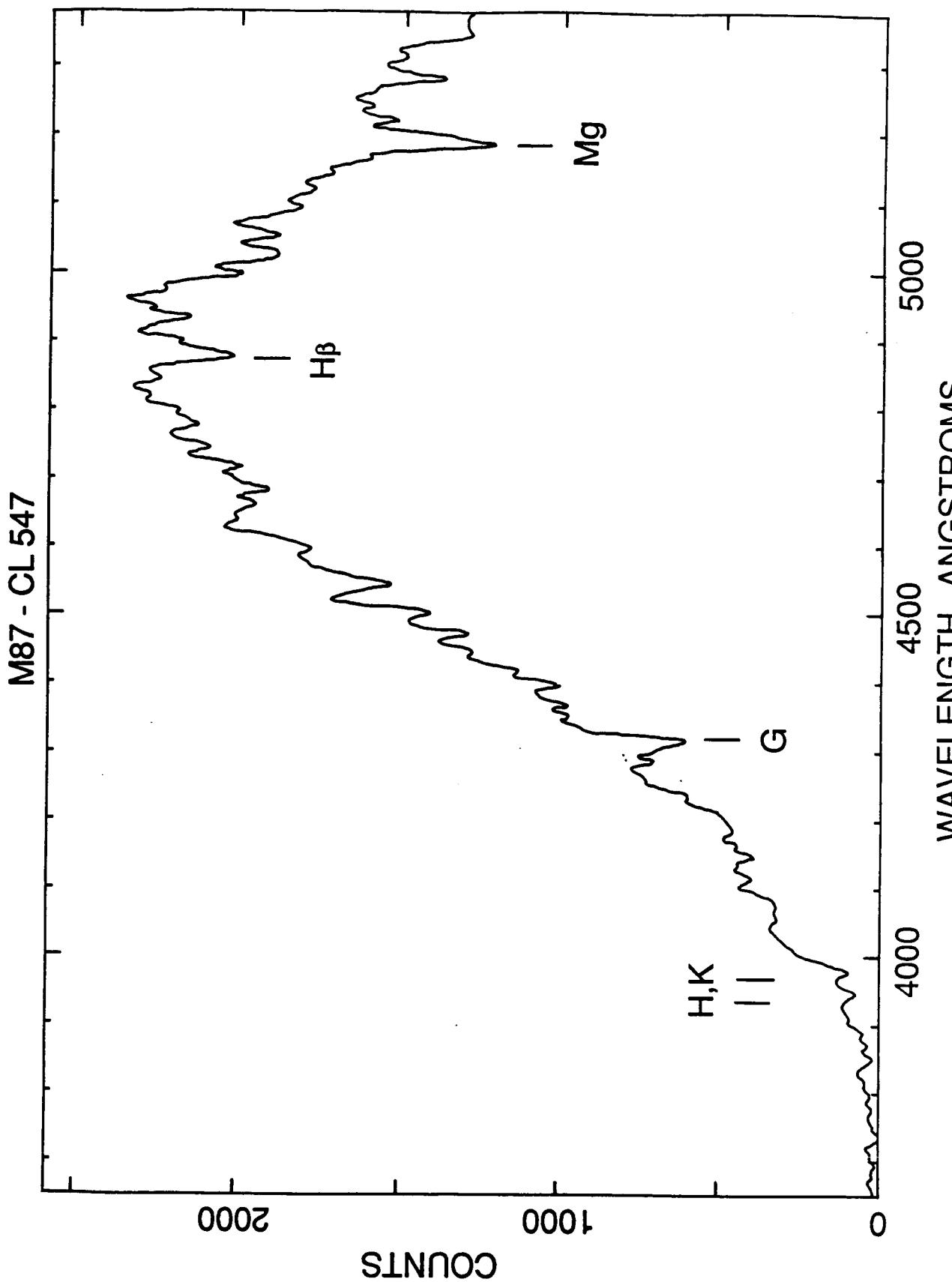
M87 - CL 547
COUNTS
0
1000
2000
4000
4500
5000
WAVELENGTH ANGSTROMS
H,K
G
Hβ
Mg

FIGURE 1

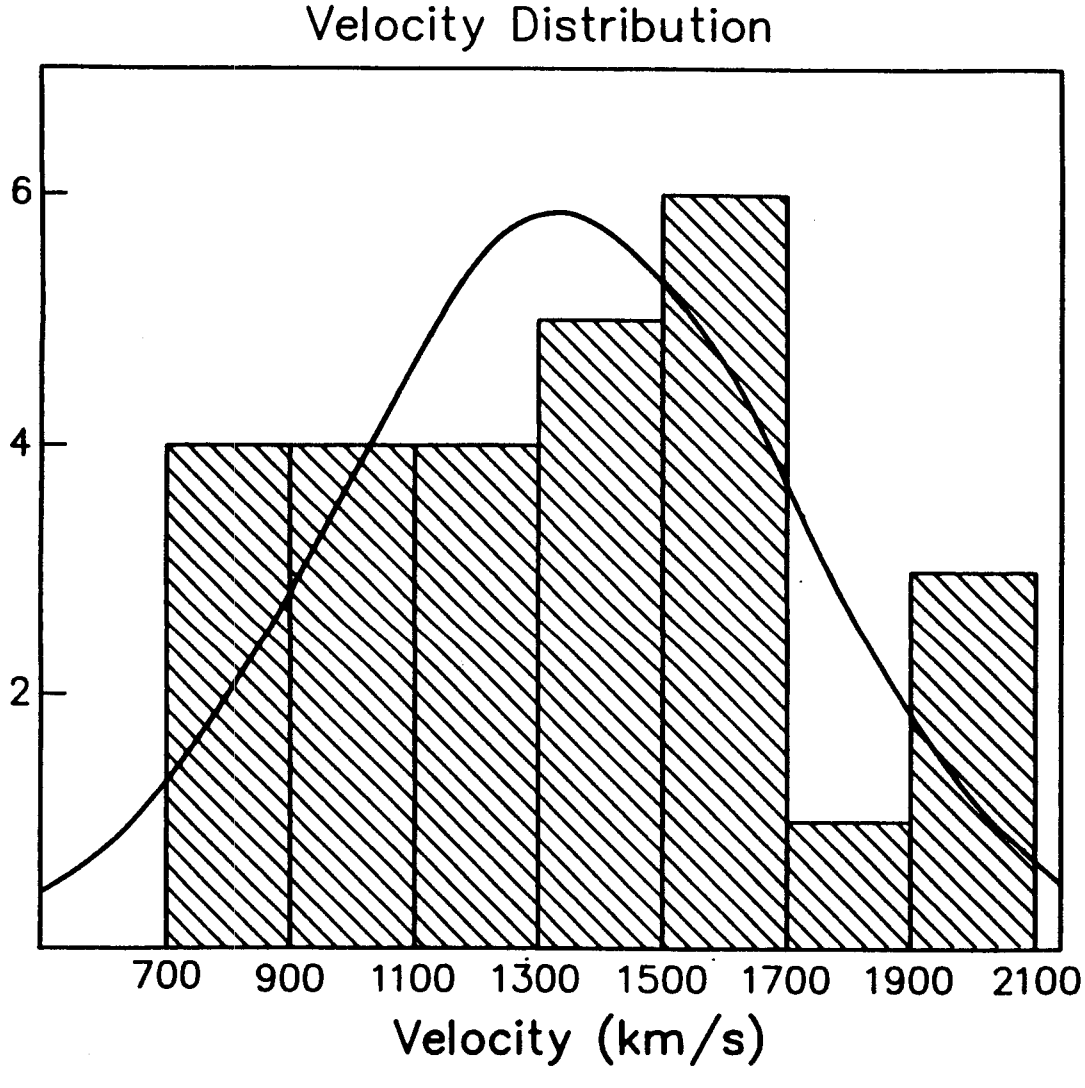
Velocity Distribution
6
4
2
700
900
1100
1300
1500
1700
1900
2100
Velocity (km/s)

FIG 1.

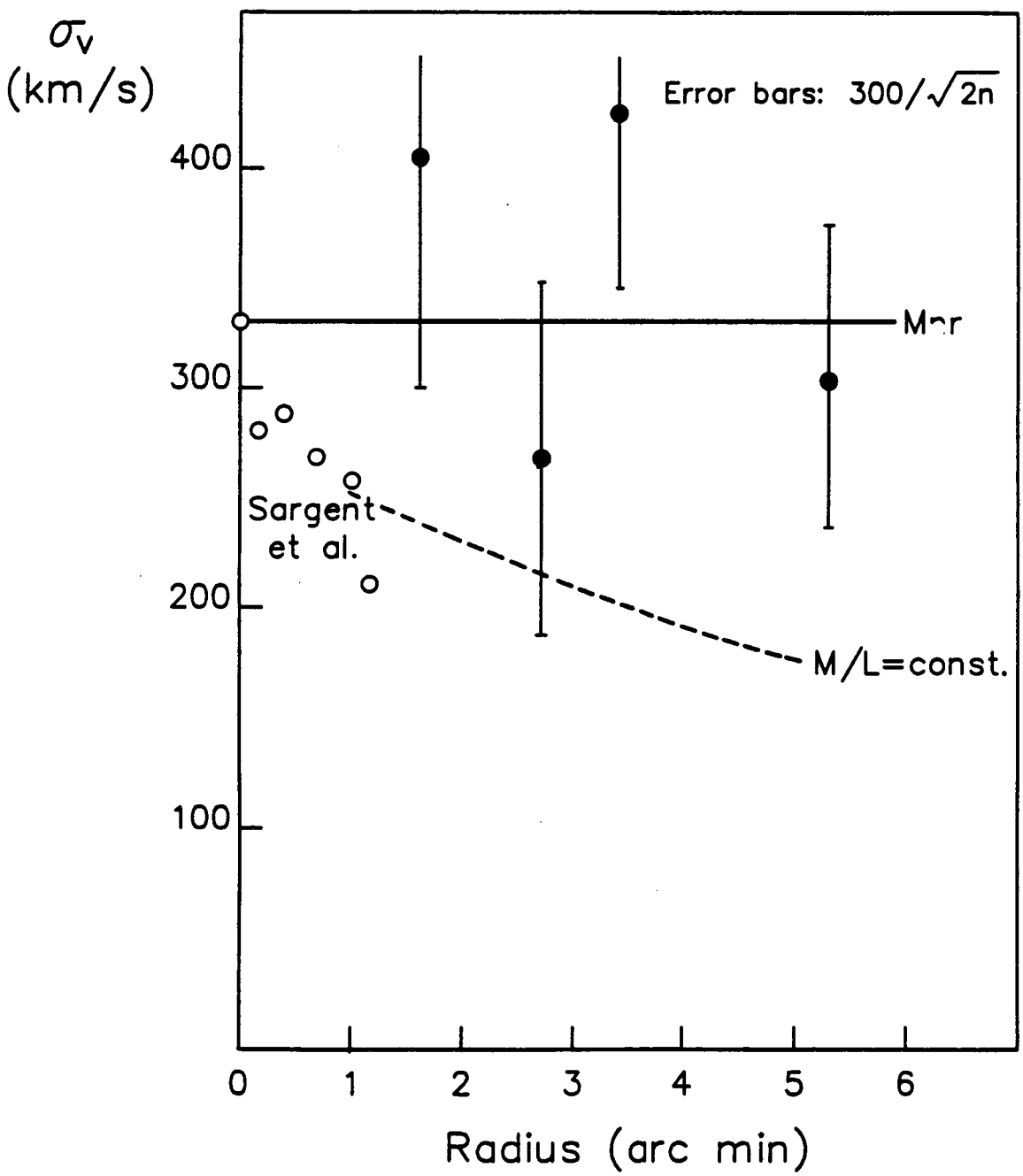
σ_v
(km/s)
Error bars: $300/\sqrt{2n}$
400
300
200
100
Sargent
et al.
M/L=const.
0
1
2
3
4
5
6
Radius (arc min)

FIG 3

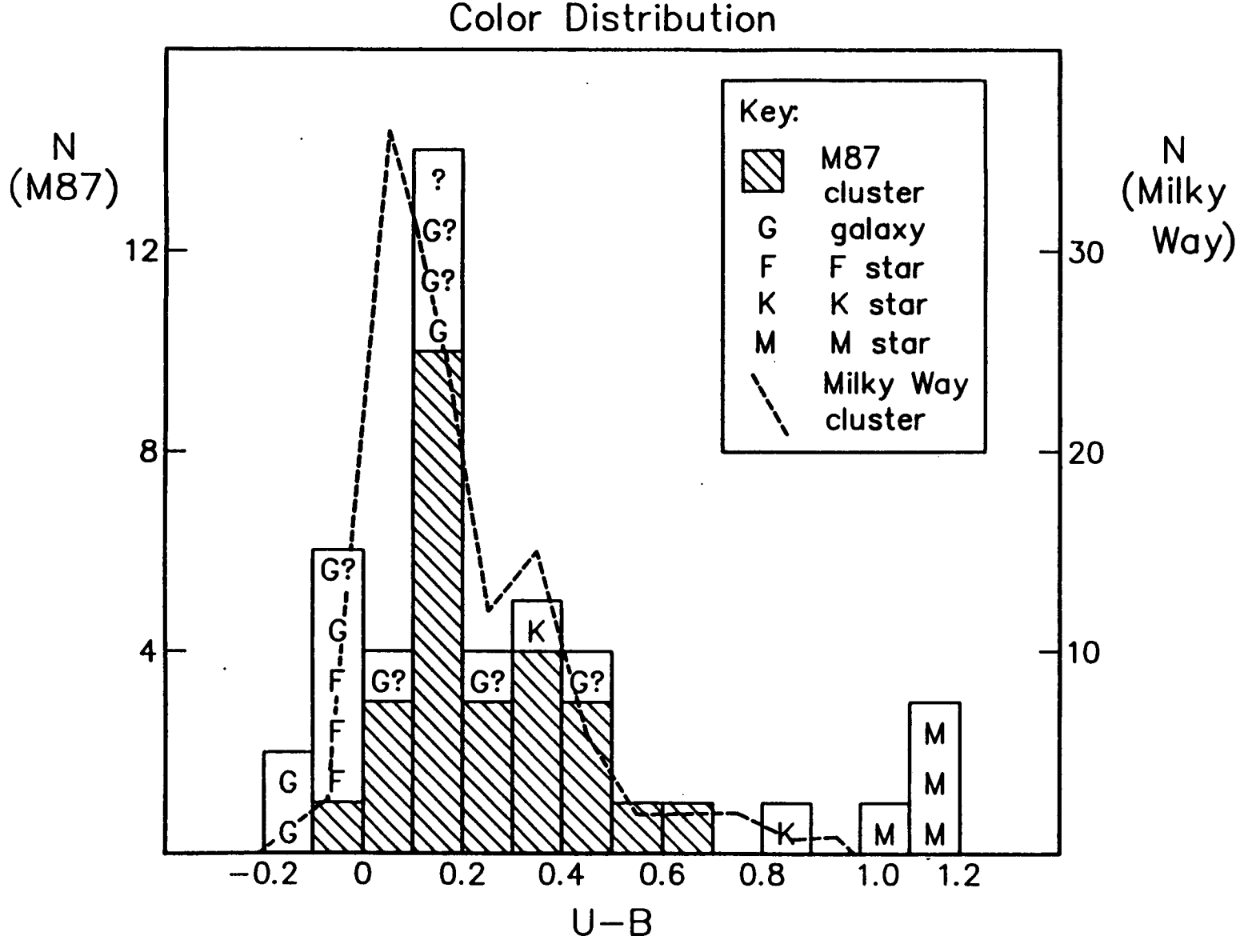
Color Distribution
N
(M87)
12
8
4
N
(Milky
Way)
30
20
10
Key:
M87
cluster
G galaxy
F F star
K K star
M M star
Milky Way
cluster
?
G?
G?
G
G?
G
F
F
F
G
G
G?
G?
G?
K
G?
K
M
M
M
M
−0.2
0
0.2
0.4
0.6
0.8
1.0
1.2
U−B

FIG 4.

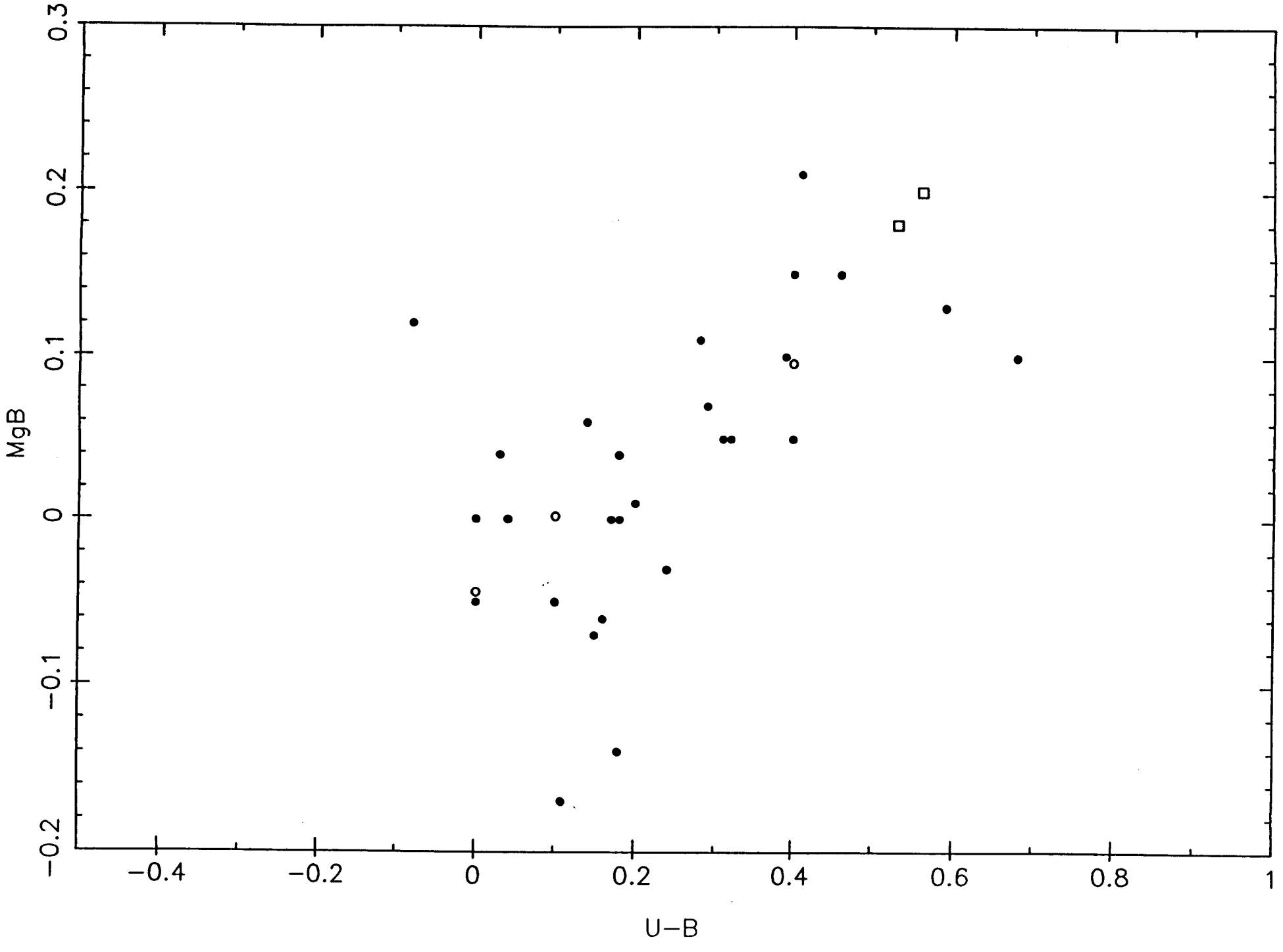

Fig 15

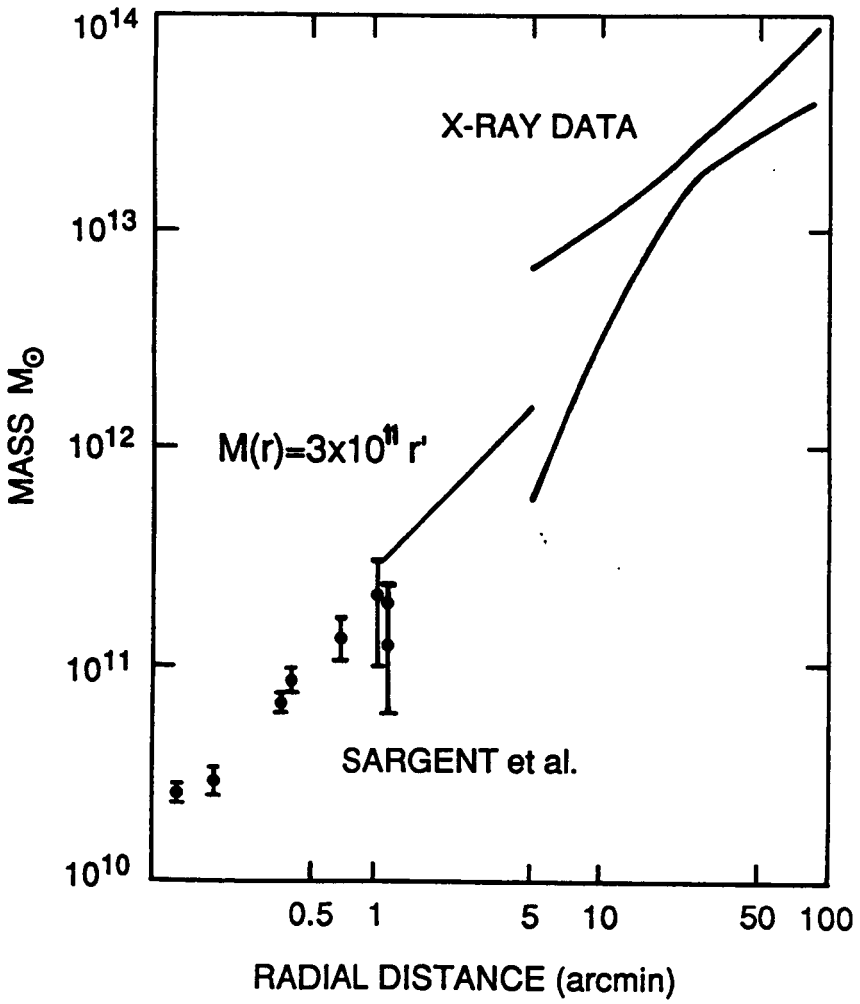
10^{14}
10^{13}
10^{12}
10^{11}
10^{10}
MASS $M_\odot$
X-RAY DATA
$M(r)=3x10^{11} r'$
SARGENT et al.
0.5
1
5
10
50
100
RADIAL DISTANCE (arcmin)

GURE 6